Effect of Small Amount of Water on CO2 Bubble Behavior in Ionic Liquid Systems

ARTICLE *in* INDUSTRIAL & ENGINEERING CHEMISTRY RESEARCH · JANUARY 2014

Impact Factor: 2.59 · DOI: 10.1021/ie40208

6 AUTHORS, INCLUDING:

Haifeng Dong
Chinese Academy of Sciences
48 PUBLICATIONS **528** CITATIONS
SEE PROFILE

X.P. Zhang
Chinese Academy of Sciences
175 PUBLICATIONS **2,662** CITATIONS
SEE PROFILE

I&EC research
Industrial & Engineering Chemistry Research

Article

pubs.acs.org/IECR

Effect of Small Amount of Water on CO_2 Bubble Behavior in Ionic Liquid Systems

Xin Zhang,[†,‡] Haifeng Dong,[†] Di Bao,[†,‡] Ying Huang,[†,‡] Xiangping Zhang,*[,†] and Suojiang Zhang*[,†]

[†]Beijing Key Laboratory of Ionic Liquids Clean Process, State Key Laboratory of Multiphase Complex System, Key Laboratory of Green Process and Engineering, Institute of Process Engineering, Chinese Academy of Sciences, Beijing, 100190, China

[‡]College of Chemistry and Chemical Engineering, University of Chinese Academy of Sciences, Beijing, 100049, China

ABSTRACT: Adding a small amount of water to ionic liquids can greatly reduce the viscosities of ionic liquids, which is believed to be an effective and economical method to make ionic liquids being applied practically for carbon capture. However, how the water content influences the bubble behavior which is used to calculate transfer properties; this is important but has not been studied systematically. In this work, the rise and deformation of single CO_2 bubbles in ionic liquids with different water contents were investigated using a high speed image pickup system. The results indicate that a small amount of water has a significant influence on the bubble behavior in ionic liquids. The viscosity plays a more important role in determining the bubble behavior than the surface tension. Two new empirical correlations verified by experimental data were proposed to predict bubble velocity and bubble diameter in different ionic liquid systems.

1. INTRODUCTION

The removal of carbon dioxide (CO_2) is considered to be a main technology for mitigating the greenhouse effect. So far, utilizing the reaction between CO_2 and aqueous solutions of alkanolamine or their mixtures to form carbamates is the most employed technology for CO_2 capture.[1−4] However, alkanolamine solutions have some drawbacks, such as volatility, corrosion, and high energy consumption. Therefore, developing new absorbents for CO_2 absorption has become a hot spot.

Ionic liquids are treated as potential candidates for CO_2 capture considering their unique characteristics, such as negligible vapor pressure, high thermal stability, tunable physicochemical characteristics, and relatively high CO_2 solubility.[5−8] However, ionic liquids commonly have high or superhigh viscosities, which leads to great resistance of mass transfer and low gas−liquid mass transfer rates.[9] Therefore, the high viscosity of ionic liquids is a major limitation for large-scale application in a continuous CO_2 capture process. In order to increase the mass transfer rate of capturing CO_2 in ionic liquids, ionic liquids were loaded on porous silica gel,[10] or the carbon capture process was intensified in a rotating packed bed contactor.[11] However, the gel loaded with ionic liquids usually shows low stability and the energy consumption is usually high for a rotating packed bed contactor. According to Seddon et al.,[12] small quantities of water could dramatically decrease the viscosity of ionic liquids which was also described in some other literature.[13,14] Based on traditional viewpoints, the mass transfer rate qualitatively increases with decreasing viscosity. Moreover, the feed gas, such as flue gas and syngas, contains some amount of water. Therefore, we prefer to mix ionic liquids with a small amount of water to increase the mass transfer rate.

Studying the bubble behavior such as bubble velocity, bubble size, and bubble deformation will provide engineering data that are necessary for engineering design and operation of industrial units using ionic liquids. The single bubble behavior conducted in conventional molecular solvents has been widely studied, such as water,[15−18] glycerin,[19,20] ethanol,[21] xanthan,[22] and silicone oil.[23] As for ionic liquids, there are few related reports. The bubble behavior in pure ionic liquids has been investigated experimentally and numerically in the literature.[24−27] However, previous study focused on pure ionic liquids, whereas the hydrodynamic research of ionic liquid blended water has not been studied.

In this work, a bubble column was selected as a gas−liquid contactor. Five different kinds of ionic liquids and their aqueous solvents were selected as liquid phases and CO_2 was selected as the gas phase, respectively. The effects of water content and other operating parameters such as temperature, gas flow rate, and orifice diameter on bubble behavior were systematically investigated. The profiles of bubble terminal velocity, bubble diameter, and bubble deformation were determined experimentally using a high speed image pickup system. Two new empirical correlations based on a wide experimental data set were proposed and verified for predicting bubble velocities and bubble diameters in different ionic liquid systems.

2. EXPERIMENTAL SECTION

2.1. Materials Preparation. Five ionic liquids were used in this study: imidazolium ionic liquids ([bmim][BF_4], [omim][BF_4], [bmim][NO_3], [bmim][$N(CN)_2$]) and pyridinium ionic liquid ([bpy][BF_4]). Before the ionic liquids were used, they were dried under vacuum for 48 h at 333 K and then kept in a drying cabinet. Karl Fischer titration shows that the water content of the ionic liquids after drying is <200 ppm. The densities and the viscosities of the ionic liquids were determined by a density meter (Anton Paar DMA 5000) with an accuracy of ±0.000 005 g·cm^{-3} and an automated

Received: July 2, 2013
Revised: November 14, 2013
Accepted: December 9, 2013
Published: December 9, 2013

dx.doi.org/10.1021/ie4020827 | *Ind. Eng. Chem. Res.* 2014, 53, 428−439

microviscometer (Anton Paar AMVn), respectively. The surface tensions were measured by the Wilhelmy plate method using a Krüss K100 tensiometer.

2.2. Experimental Setup and Procedure. The experiments were carried out using a similar bubble column employed by our research team.[24] All experiments were conducted at temperatures ranging from 303 to 343 K and at ambient pressure. The CO_2 gas was injected via an orifice. Three different stainless steel orifices were adopted in the present work with inner diameters 0.47, 0.8, and 1.4 mm, respectively. The water contents of ionic liquids were determined by the Karl Fischer titration method after the addition of a certain amount of deionized water to freshly prepared ionic liquids. Detailed experimental procedures and the description of the image pickup system can be seen in our previous work.[27]

2.3. Image Analysis and Measurement Accuracy. The significant bubble geometrical and motional parameters, namely the vertical and horizontal diameters, and the centroid coordinate (x, y) of the bubble were obtained with Image Pro Plus software. The local velocity V_i at a given distance L from the centroid of the first bubble leaving the orifice was determined by eqs 1 and 2.

$$L = \sqrt{(x_i - x_0)^2 + (y_i - y_0)^2} \tag{1}$$

$$V_i = \frac{\sqrt{(x_i - x_{i-1})^2 + (y_i - y_{i-1})^2}}{\Delta t} \tag{2}$$

where (x_i, y_i) and (x_{i-1}, y_{i-1}) are the coordinates of the sequential bubble positions and Δt means the time interval of two successive pictures, which equals 0.002 s in present study.

Bubbles are supposed to be ellipsoids. The bubble equivalent diameter d_{eq} is defined as a sphere with the same volume as an ellipsoid which can be calculated by the following equations:[28]

$$\frac{4}{3}\pi {d_{eq}}^3 = \frac{4}{3}\pi {d_h}^2 d_v \tag{3}$$

$$d_{eq} = \sqrt[3]{{d_h}^2 d_v} \tag{4}$$

where d_v and d_h are the vertical and horizontal diameters, respectively.

The aspect ratio, E, which describes the bubble deformation, is defined as the ratio between the vertical and horizontal diameters of the bubble. The aspect ratio of spherical bubble equals 1, while other kinds of bubbles are always less than 1.

$$E = \frac{d_v}{d_h} \tag{5}$$

For calibrating the measurement system, a graduated scale with the same focal distance as the measured bubbles was attached to the column. The minimum measurable length is 0.02 mm after performance of the calibration of the measurement system. The minimum observed bubble is about 1.5 mm in the present work. Therefore the measurement uncertainty is less than 2%.

3. RESULTS AND DISCUSSION

3.1. Physical Properties of Ionic Liquids. The physical properties of ionic liquids, namely density, viscosity, and surface tension are depicted in Figures 1−4. Detailed values at 303 K are presented in Table 1. The density of an ionic liquid is well fitted with a linearly decreasing function of water content, while the surface tension increases approximate linearly with increasing water content. Compared with density and surface

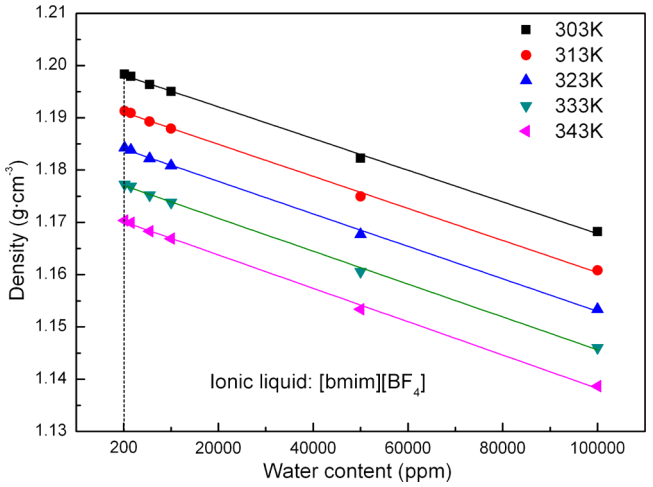

Figure 1. Density of ionic liquid at varying water contents and temperatures.

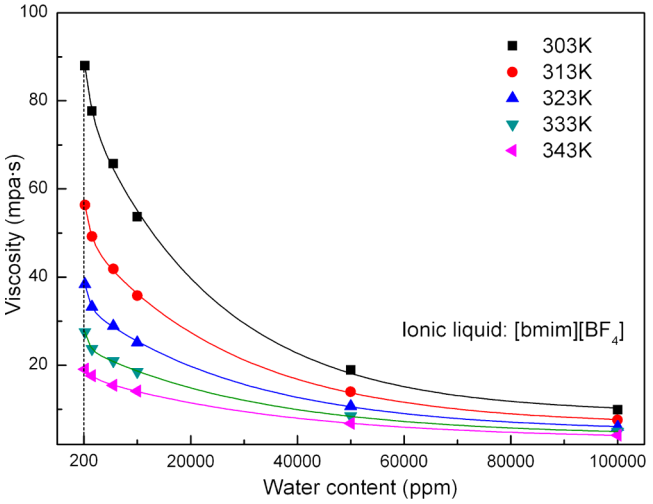

Figure 2. Viscosity of ionic liquid at varying water contents and temperatures.

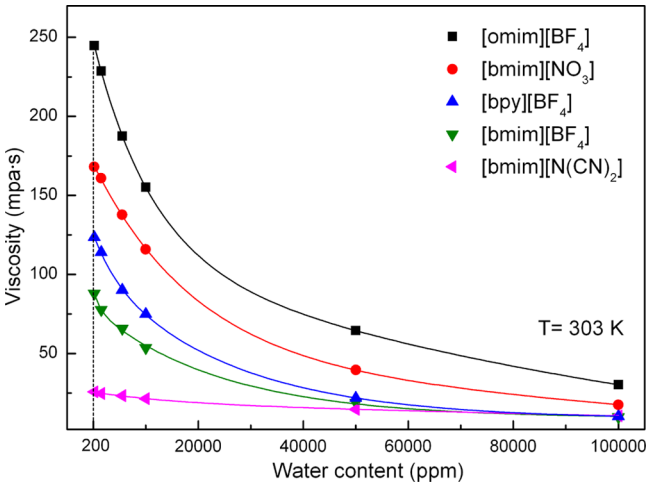

Figure 3. Viscosity of different ionic liquids at varying water contents.

dx.doi.org/10.1021/ie4020827 | Ind. Eng. Chem. Res. 2014, 53, 428−439

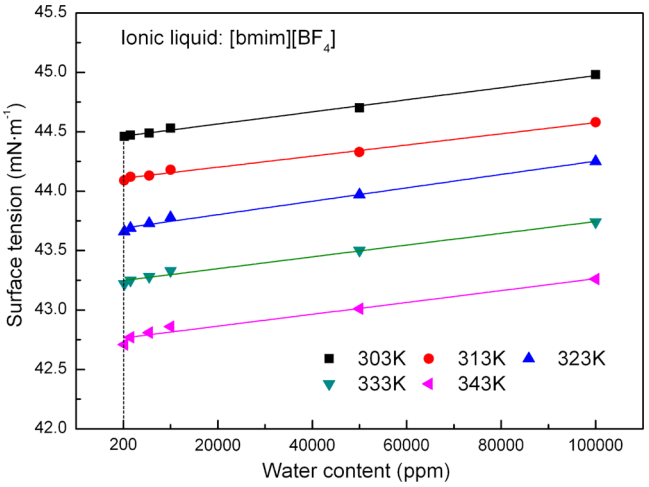

Figure 4. Surface tension of ionic liquid at varying waters contents and temperatures.

Table 1. Effect of Water Content on Physical Properties of Different Ionic Liquids at 303 K

ionic liquid	water content (ppm)	ρ_l (g/cm^3)	μ_l (mPa s)	σ (mN/m)
[bmim][BF_4]	200	1.198 363	87.9756	44.46
[bmim][BF_4]	1 500	1.197 967	77.6902	44.47
[bmim][BF_4]	5 500	1.196 371	65.7631	44.49
[bmim][BF_4]	10 000	1.195 045	53.6844	44.53
[bmim][BF_4]	50 000	1.182 270	18.9052	44.70
[bmim][BF_4]	100 000	1.168 229	9.8627	44.98
[omim][BF_4]	10 000	1.098 841	155.2252	33.14
[bmim][NO_3]	10 000	1.156 205	115.8977	49.63
[bpy][BF_4]	10 000	1.207 911	74.924	45.59
[bmim][$N(CN)_2$]	10 000	1.057 86	21.45	44.64

tension, water has a more obvious impact on the viscosity of ionic liquid. Adding a small amount of water can sharply reduce the viscosity of an ionic liquid. Figure 2 also shows that the tendency of viscosity reduction slows down with continuously adding water to ionic liquid. When the water content is over 50 000 ppm (weight ratio), the viscosity will no longer decrease remarkably. Therefore, the specific water contents chosen in the present study (200−100 000 ppm) cover a wide range of physical properties of ionic liquid, and further comprehensively reflect the bubble behavior in ionic liquids.

The micromechanism of the water effect on the structure of ionic liquids was illustrated in the literature.[29] In aqueous ionic liquid, the molecular mass of water is generally much less than that of the ions it replaces. These lighter water molecules tend to displace much heavier counterions from the ion coordination shells, weakening the ion−ion correlations. This reduces caging and increases the diffusivity, which leads to higher conductivities and lower viscosities.

For ionic liquids, different anion and cation combinations will present remarkable differences in individual physical properties. Five specific ionic liquids were selected in this work owing to their partly same ions but different physical properties, especially the viscosity, which could be verified in Figure 3. Comparing [bmim][BF_4] and [omim][BF_4], they have the same anion but different cations. According to the literature,[30] the van der Waals interaction increases with increasing the alkyl side chain length of ionic liquids. Therefore, the viscosity of ionic liquids increases with an increase of the length of the alkyl side chain. As for [bmim][BF_4] and [bpy][BF_4], the viscosities of ionic liquids with six-membered-ring cations, $[py]^+$, are larger than those with five-membered-ring cations, $[im]^+$. Concerning the ionic liquids with the same cation ([bmim][BF_4], [bmim][NO_3], and [bmim][$N(CN)_2$]), viscosity increases in the order $[N(CN)_2]^- < [BF_4]^- < [NO_3]^-$. The lower viscosity of the ionic liquid with the $[N(CN)_2]^-$ anion is interpreted by the more delocalized negative charge distribution on the anion and the weaker cation−anion charge interaction. The higher viscosities for other two anions are attributed to the more rigid structures and the lack of conformational degrees of freedom.[31]

3.2. Bubble Velocity. *3.2.1. Factors Affecting the Bubble Velocity.* Bubble velocities in ionic liquid systems were obtained with eqs 1 and 2. Figure 5 presents the profile of

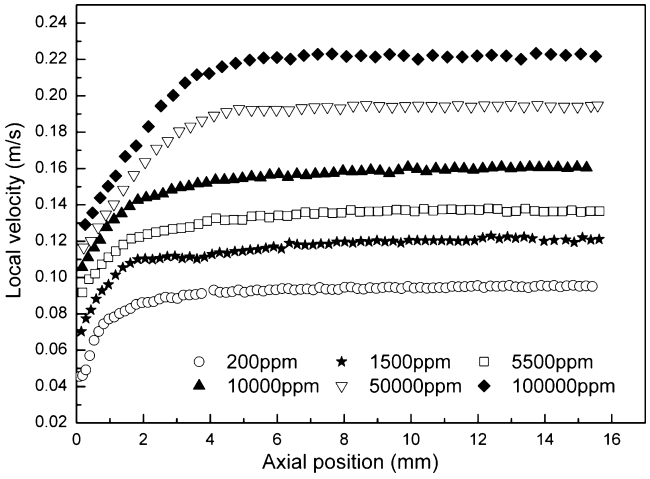

Figure 5. Bubble local velocity in [bmim][BF_4] with different water contents (Q_{in} = 0.89 mL/min, T = 333 K, D_o = 0.47 mm).

bubble local velocity at different water contents as a function of axial position of the bubble column. It shows that, after a short distance for acceleration, the bubble local velocity quickly remains unchanged which means that the bubble has reached the terminal velocity. When the water content is increased, the distance of bubble acceleration increases as well. The bubble terminal velocity is 0.22 m/s at 100 000 ppm compared with 0.09 m/s at 200 ppm. The viscosity of ionic liquid decreases when the water content is increased. Therefore, the bubble terminal velocity increases with an increase of water content in ionic liquid.

The influence of temperature on bubble local velocity is presented in Figure 6. It shows results similar to those of Figure 5. The bubble terminal velocity is higher when the liquid temperature is increased. This can also be ascribed to the fact that the viscosity of ionic liquid reduces as the liquid temperature increases. Detailed data points of the bubble terminal velocity as a function of the water content at different temperatures are depicted in Figure 7. The results clearly demonstrate that bubble terminal velocity increases with an increase of water content and temperature in ionic liquid. The bubble terminal velocity increases faster at lower water content, while the increasing rate gets lower as the water content increases. This result agrees well with the previous discussion in Figure 2 and Table 1. Initially, the viscosity of ionic liquid reduces dramatically with the addition of a very small amount

dx.doi.org/10.1021/ie4020827 | Ind. Eng. Chem. Res. 2014, 53, 428−439

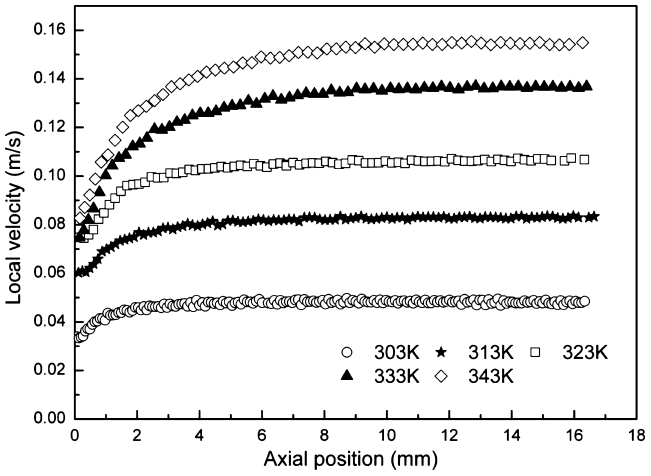

Figure 6. Bubble local velocity in [bmim][BF_4] at different temperatures (Q_{in} = 0.25 mL/min, D_o = 0.47 mm, water content = 200 ppm).

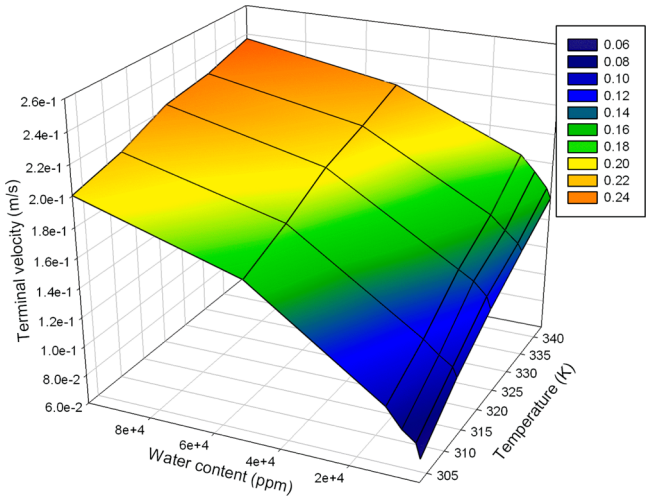

Figure 7. Bubble terminal velocity in [bmim][BF_4] at varying water contents and temperatures (Q_{in} = 2.17 mL/min, D_o = 0.47 mm).

of water. Then, the trend of viscosity reduction slows down with continuous addition of water to ionic liquid.

It can be seen from Figure 8 that the order of the bubble terminal velocity in different ionic liquids is [omim][BF_4] < [bmim][NO_3] < [bpy][BF_4] < [bmim][BF_4] < [bmim][N-$(CN)_2$], which is in the reverse order of viscosity values in these ionic liquid systems. According to Table 1, the differences of surface tension in the studied ionic liquid systems are much less than those of viscosity. Therefore, viscosity has a more significant effect on the bubble behavior in ionic liquid systems in comparison with surface tension.

The influence of orifice diameter and gas flow rate on bubble velocity was also investigated, as shown in Figure 9. The results demonstrate that the increase of gas inlet flow rate or orifice diameter enhances the bubble terminal velocity. High gas flow rates favor the coalescence of single bubbles before detaching from the orifice. Therefore, it is reasonable to find that bubble velocity increases with an increase of the gas flow rate. As for the orifice diameter, larger bubbles will be formed with an increase of orifice diameter which leads to a greater buoyancy force of the bubbles in ionic liquid systems.

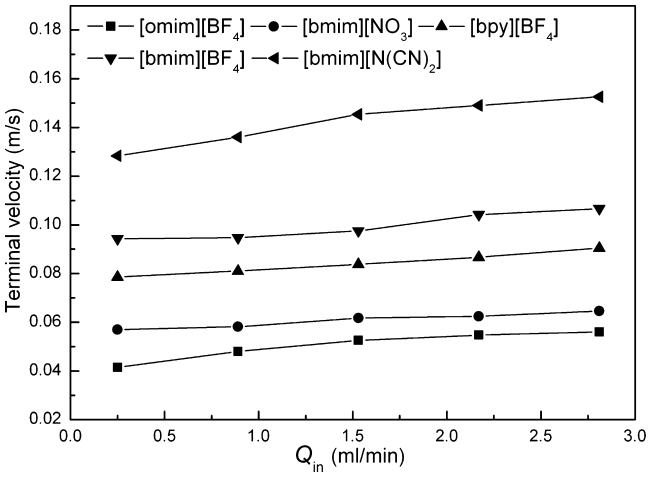

Figure 8. Bubble terminal velocity at at different gas flow rates (T = 333 K, water content = 200 ppm).

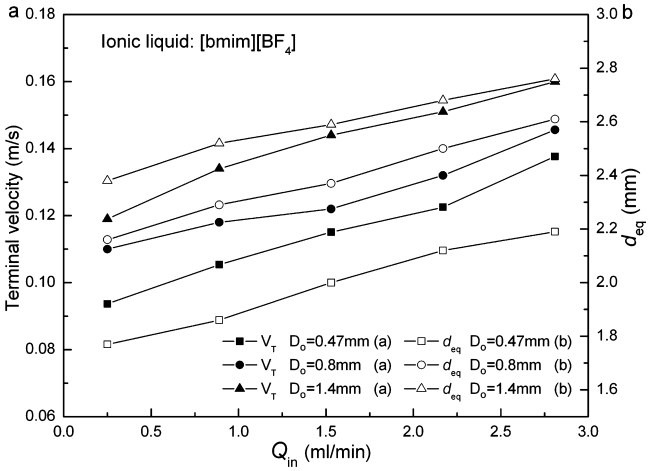

Figure 9. Bubble terminal velocity and bubble diameter at varying orifice diameters and gas flow rates (T = 333 K, water content = 200 ppm).

Table 2. Range of Investigated Dimensionless Parameters in Present Study

param	max	min
Re	146	1.09
Mo	0.142	2.96×10^{-8}
Eo	3.14	0.92

3.2.2. Bubble Velocity Correlation. Studying the bubble rise velocity in ionic liquid systems can provide important information on the overall hydrodynamics of the system. The present study covers a wide range of physical properties of ionic liquids represented by dimensionless parameters shown in Table 2. Many investigators developed empirical or semi-empirical correlations to predict the bubble rising velocity. Mendelson[32] proposed a wave theory in which the surfaces were considered to be rigid. According to the wave theory, the bubble terminal velocity can be directly calculated by the following equation:

$$V_T = \sqrt{\frac{2\sigma}{d_{eq}\rho_l} + \frac{(\rho_l - \rho_g)g d_{eq}}{2\rho_l}} \quad (6)$$

dx.doi.org/10.1021/ie4020827 | Ind. Eng. Chem. Res. 2014, 53, 428−439

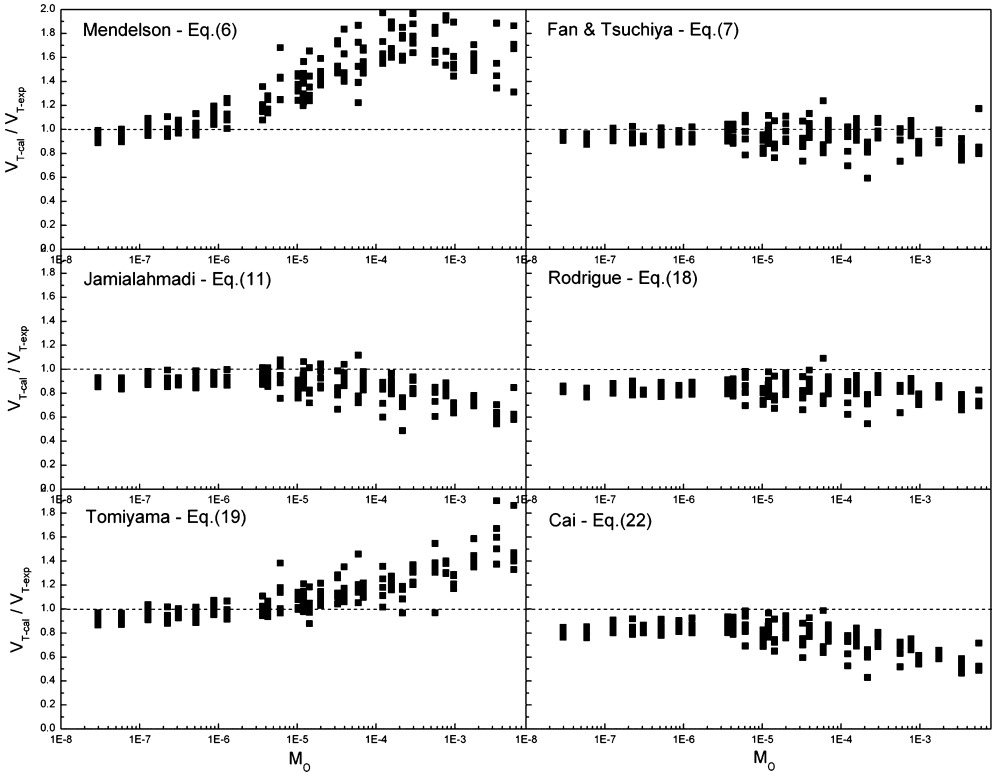

Figure 10. Predictions of bubble terminal velocity in ionic liquid systems using models from the literature as a function of Morton number.

where V_T is the terminal velocity, d_{eq} is the bubble equivalent diameter, ρ_l is the liquid density, ρ_g is the gas density, and σ is the surface tension.

Another general correlation for the prediction of bubble terminal velocity which may be applied to both pure and contaminated systems was proposed by Fan and Tsuchiya.[33] The equations are interpreted as follows:

$$V_T = (V_{T1}^{-n} + V_{T2}^{-n})^{-1/n} \tag{7}$$

$$V_{T1} = \frac{\rho_l g d_{eq}^{\ 2}}{K_b \mu_l} \tag{8}$$

$$V_{T2} = \sqrt{\frac{2c\sigma}{d_{eq}\rho_l} + \frac{g d_{eq}}{2}} \tag{9}$$

where V_{T1} and V_{T2} are the expressions for terminal velocity in the viscous regime and in the distorted or cap bubble regime. The three parameters n, c, and K_b reflect three specific factors governing the rate of bubble rising.

$$K_b = \max(12, K_{bo} Mo^{-0.038}) \tag{10}$$

where K_{bo} equals 14.7 for aqueous solutions and 10.2 for organic solvents or mixtures. As for the other two parameters, the recommended values of 1.6 for n and 1.4 for c were adopted in the present study.

Jamialahmadi et al.[34] studied the wave analogy and provided the following equations to predict the bubble rising velocity in pure liquids:

$$V_T = \frac{V_b V_T^W}{\sqrt{(V_b)^2 + (V_T^W)^2}} \tag{11}$$

$$V_b = \frac{1}{18}\frac{\rho_l - \rho_g}{\mu_l} g d_{eq}^{\ 2} \tag{12}$$

$$V_T^W = \sqrt{\frac{2\sigma}{d_{eq}(\rho_l + \rho_g)} + \frac{g d_{eq}}{2}} \tag{13}$$

where V_b is the bubble rising velocity of a spherical bubble, V_T^W is the traveling wave velocity in front of the bubble, and V_T is the terminal rising velocity coupled by the two velocities.

Rodrigue[35] discussed the motion of single bubbles rising steadily in pure Newtonian liquids, such as water, olive oil, and glycerin and proposed a correlation based on most of the published data. Rodrigue[35] introduced two new dimensionless numbers, namely the flow number (F) and the velocity number (U), defined as

$$F = g\left[\frac{d_{eq}^{\ 8}\rho_l^{\ 5}}{\sigma \mu_l^{\ 4}}\right]^{1/3} = Eo\left(\frac{Re}{Ca}\right)^{2/3} \tag{14}$$

$$U = V_T\left[\frac{d_{eq}^{\ 2}\rho_l^{\ 2}}{\sigma \mu_l}\right]^{1/3} = (Re^2 Ca)^{1/3} \tag{15}$$

where Ca, Eo, Re are the capillary number, the Eötvös number, and the Reynolds number, respectively. Furthermore, the bubble terminal velocity can be obtained through the calculations of eqs 16 − 18.

$$U = \frac{0.0833F}{1 + 0.049F^{0.75}} \tag{16}$$

dx.doi.org/10.1021/ie4020827 | Ind. Eng. Chem. Res. 2014, 53, 428−439

$$V_T\left[\frac{d_{eq}^{\ 2}\rho_l^{\ 2}}{\sigma\mu_l}\right]^{1/3} = \frac{0.0833F}{1 + 0.049F^{0.75}} \quad (17)$$

$$V_T = \frac{0.0833F}{1 + 0.049F^{0.75}}\left[\frac{d_{eq}^{\ 2}\rho_l^{\ 2}}{\sigma\mu_l}\right]^{-1/3} \quad (18)$$

Tomiyama et al.[36] developed a new generalized correlation for the prediction of the terminal velocity of bubbles. The aspect ratio was introduced because the bubbles were considered as distorted oblate spheroids. In this model, bubbles were further assumed to be symmetric ellipsoids and the following expression for V_T was obtained.

$$V_T = \frac{\sin^{-1}(1 - E^2)^{1/2} - E(1 - E^2)^{1/2}}{1 - E^2}\left[\frac{8\sigma}{d_{eq}\rho_l}E^{4/3} + \frac{(\rho_l - \rho_g)gd_{eq}}{2\rho_l}\frac{E^{2/3}}{1 - E^2}\right]^{1/2} \quad (19)$$

Recently, Cai et al.[37] investigated the rising behavior of single bubbles in six systems with a wide range of Morton numbers from 3.21×10^{-11} to 163. The results show that the new correlation for predicting the bubble rising velocity is valid in high viscous liquids with viscosity up to 1.515 Pa s.

$$V_b = 0.417d_{eq}^{\ 1.83}\left(\frac{\mu_l}{\rho_l}\right)^{-0.886}Mo^{-0.028} \quad (20)$$

$$V_T^W = \sqrt{\frac{2\sigma}{d_{eq}(\rho_l + \rho_g)} + \frac{gd_{eq}}{2}} \quad (21)$$

$$V_T = V_b\left[\left(\frac{V_b}{V_T^W}\right)^{2.2} + 1\right]^{-0.5} \quad (22)$$

These typical and significant correlations that depicted above are selected, namely eqs 6−22. Their predictions for ionic liquid systems were compared with the experimental data in Figure 10, which shows the ratio between calculated and experimental bubble terminal velocities versus the Morton number. The predictions for ionic liquid systems calculated by eq 6 exhibit a large error, up to +100% with an increase of Morton number. The Fan and Tsuchiya correlation, eq 7, presents the relatively most proximate estimation with an overestimation within +25% and an underestimation within −35%. The predictions of eq 11 present a big deviation over the entire range with a relative error from +10% to −50%. The Rodrigue correlation, eq 18, shows a similar tendency calculated by eq 11 with an underestimation up to −45%. The correlation of eq 19 presents relatively accurate results at low *Mo* but largely overestimates ionic liquid data at high *Mo*. Finally, eq 22 does not fit the experimental data in ionic liquid systems as well, which shows a big underestimation within −55%.

As described above, these correlations which fit very well in molecular solvents cannot be directly applied to predict the bubble velocity in ionic liquid systems. This may be attributed to the specific structure of the gas−liquid interface in ionic liquids. According to the literature,[38] the interface of ionic liquids is populated by both anions and cations with no segregation and the cation ring is perpendicular rather than parallel to the surface, which is intrinsically different from molecular solvents.

It is comprehensively reported in the literature[39] that bubble terminal velocity depends on different variables: bubble diameter, gas density, liquid density, liquid viscosity, and liquid surface tension. Therefore, the correlation should be developed within these variables. A general function f is proposed, which satisfies:

$$f(d_{eq}, \rho_l, \rho_g, \mu_l, \sigma, V_T, g) = 0 \quad (23)$$

Two dimensionless groups, the Morton number and the Eötvös number, were selected in the present study, defined as follows:

$$Mo = \frac{g\mu_l^{\ 4}(\rho_l - \rho_g)}{\sigma^3\rho_l^{\ 2}} \quad (24)$$

$$Eo = \frac{\rho_l g d_{eq}^{\ 2}}{\sigma} \quad (25)$$

Then the correlation was supposed with the following form:

$$V_T\left[\frac{d_{eq}^{\ 2}(\rho_l - \rho_g)^2}{\sigma\mu_l}\right]^{1/3} = aMo^bEo^c \quad (26)$$

Adopting the least-squares method, the value of each parameter is obtained: $a = 0.355$, $b = -0.172$, and $c = 0.548$. Finally, the empirical correlation for the bubble terminal velocity in a bubble column operating with ionic liquids reads as follows:

$$V_T\left[\frac{d_{eq}^{\ 2}(\rho_l - \rho_g)^2}{\sigma\mu_l}\right]^{1/3} = 0.355Mo^{-0.172}Eo^{0.548} \quad (27)$$

As shown in Figure 11, the calculated bubble terminal velocities by eq 27 are randomly distributed along the diagonal $V_T^{cal} = V_T^{exp}$. Figure 11 also clearly demonstrates that the majority of the deviations are within ±10%. The new correlation presents high simplicity and efficiency in computing bubble terminal velocities for different ionic liquid systems.

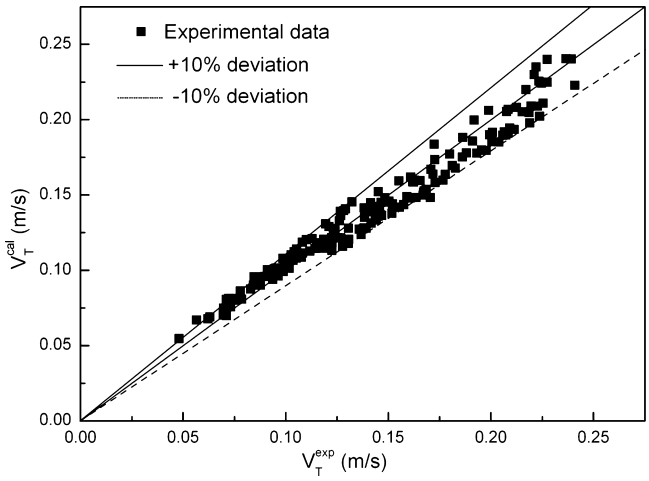

Figure 11. Comparison between predicted and measured bubble terminal velocities in ionic liquid systems.

dx.doi.org/10.1021/ie4020827 | *Ind. Eng. Chem. Res.* 2014, 53, 428−439

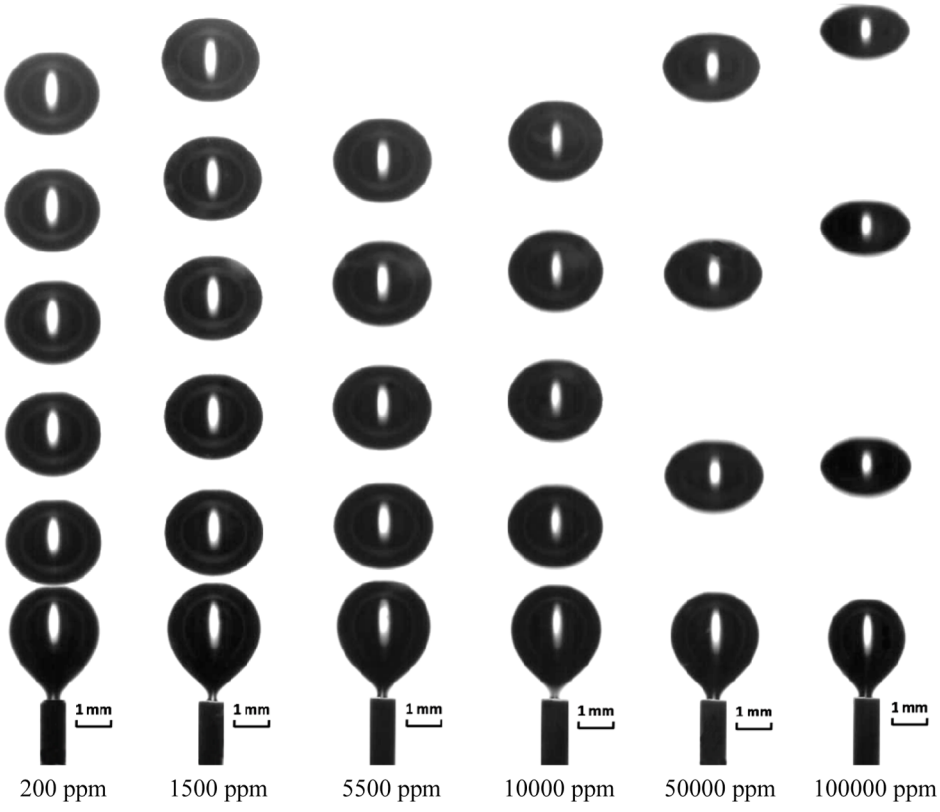

Figure 12. Effect of water content on the same bubble motion in [bmim][BF_4] (T = 313 K, D_o = 0.47 mm, Q_{in} = 0.89 mL/min).

3.3. Bubble Diameter and Bubble Deformation. *3.3.1. Factors Affecting the Bubble Diameter.* The bubble equivalent diameters in ionic liquid systems were measured at different water contents ranging from 200 to 100 000 ppm. The liquid temperature, gas flow rate, and orifice diameter were held constantly at 313 K, 0.89 mL/min, and 0.47 mm, respectively. Six typical images of the same bubble motion in ionic liquids at different water contents are shown in Figure 12. The time intervals between any two adjacent bubbles are all 0.034 s. Figure 12 shows that adding a small amount of water has a remarkable effect on the bubble behavior in ionic liquids. Bubbles are spherical or nearly spherical when the water content is low. With an increase of water content, bubbles become flatter and more like an ellipsoid. The images also show that bubble diameters decrease when the water content is increased. It can be explained with Table 1, since viscosity decreases while surface tension increases as the water content in ionic liquids increases. For the viscous media like ionic liquids, big bubbles are more likely to form directly at the orifice when the viscosity is high. However, according to Sardeing et al.,[40] the bubble diameter will increase as the surface tension value increases. Therefore, viscosity and surface tension compete with each other for the bubble diameter determination in ionic liquids. The variation of the viscosity is much larger than that of the surface tension during the same water content range. Therefore, it is reasonable to deduce that the viscosity plays a more leading role in bubble diameter determination in comparison with the surface tension.

As depicted from Figures 1−4, the physical properties of ionic liquids, especially the viscosity, is significantly influenced by temperature. For [bmim][BF_4] + 0.02% H_2O solvent, the value of viscosity at 343 K is only 1/4 that at 303 K. Moreover, when the water content in ionic liquids is increased, the influence of temperature on the physical properties decreases. It is reported that, in the carbon capture system, the inlet temperature of the solvents is usually kept at 313 K after considering the absorbing rate and capacity.[41] However, as for the [bmim][BF_4] + 0.02% H_2O solvent, the viscosity is 56.35 mPa s at 313 K, which is still too viscous for CO_2 capture. When 5 wt % water is added to ionic liquids at 313 K, the viscosity sharply decreases to 13.94 mPa s, which will no doubt considerably enhance the mass transfer rates. Therefore, adding a small amount of water is an efficient and economical way to decrease the viscosity of ionic liquid.

Figure 13 shows the influence of gas flow rates and ionic liquid temperatures on bubble equivalent diameters. It is observed that bubble equivalent diameters increase with an increase of gas flow rate as well as with the decrease of temperature, namely, with an increase of viscosity. A similar observation was also reported by Snabre and Magnifotcham[20] for the air−glycerin system.

3.3.2. Factors Affecting the Bubble Deformation. Figure 12 presents the real bubble motion in ionic liquid systems. Initially, bubble forms and grows at the orifice and then bubble moves upward following a straight trajectory after departure from the orifice. When a bubble is rising freely in ionic liquid systems, the main forces experienced by a bubble are buoyancy, drag force, added mass force, and Basset force. Bubble shape is controlled by the balance of the mentioned forces. The aspect ratio, E, is introduced in this work to represent the degree of bubble deformation in ionic liquid systems. Figure 14 presents the bubble deformation tendency on the bubble rising trajectory at different water contents. According to Figure 14, bubble aspect ratio decreases with an increase of the water content. In each case, the bubbles formed at the orifice are all spherical or nearly spherical, which means that the aspect ratio

dx.doi.org/10.1021/ie4020827 | Ind. Eng. Chem. Res. 2014, 53, 428−439

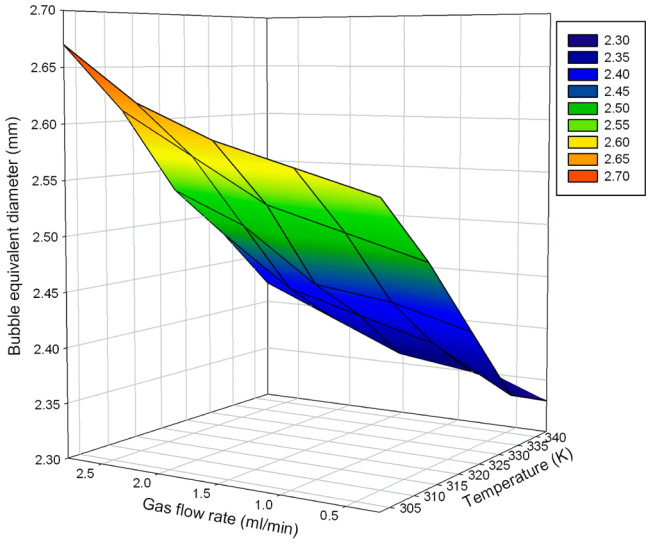

Figure 13. Bubble diameter in [bmim][BF_4] at varying gas flow rates and temperatures (water content = 10 000 ppm, D_o = 0.47 mm).

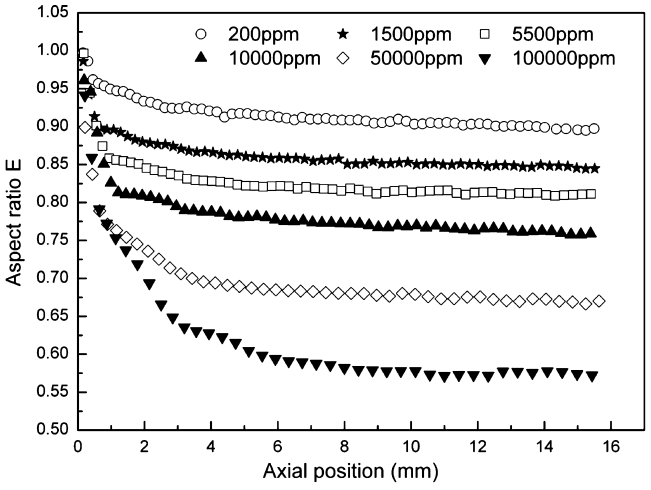

Figure 14. Bubble deformation in [bmim][BF_4] at varying water contents (Q_{in} = 2.17 mL/min, T = 323 K, D_o = 0.47 mm).

is close to 1. However, after departure from the tip of the orifice, the bubble's shape changes greatly in a very short time. The results also demonstrate that when bubbles reach terminal velocities, bubbles at 200 ppm are still nearly spherical but bubbles at 100 000 ppm turn to very flat ellipsoids. In other words, bubbles' shapes change much greater at higher water content, namely, at lower viscosity of ionic liquids, which can be verified in Figure 12.

The influence of temperature on bubble aspect ratio is shown in Figure 15. The bubble aspect ratio decreases with an increase of the liquid temperature. Comparing Figure 14 with Figure 15, the bubble aspect ratio approaches the constant just in 6 mm above the orifice, which is almost the same distance for the bubble to achieve terminal velocity. Therefore, when a bubble reaches its terminal velocity in ionic liquid systems, the bubble shape will no longer change as well. Figure 16 shows detailed data describing the aspect ratio of the bubble which has reached terminal velocity at different water contents and liquid temperatures. It shows that the aspect ratio decreases with an increase of water content and liquid temperature, which is in agreement with previous analysis.

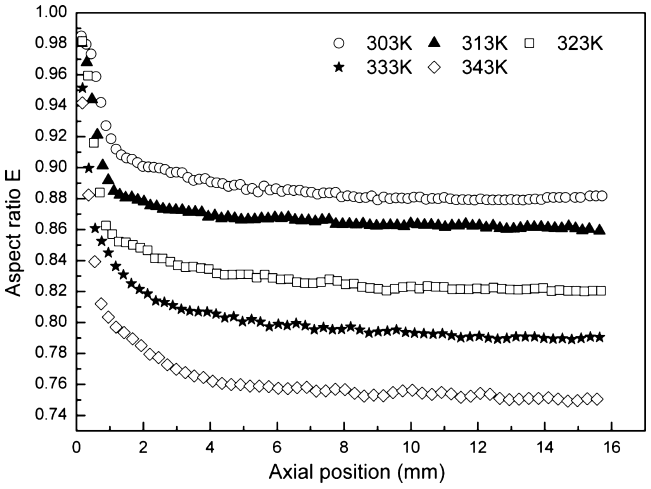

Figure 15. Bubble deformation in [bmim][BF_4] at varying temperatures (Q_{in} = 0.89 mL/min, D_o = 0.47 mm, water content = 5500 ppm).

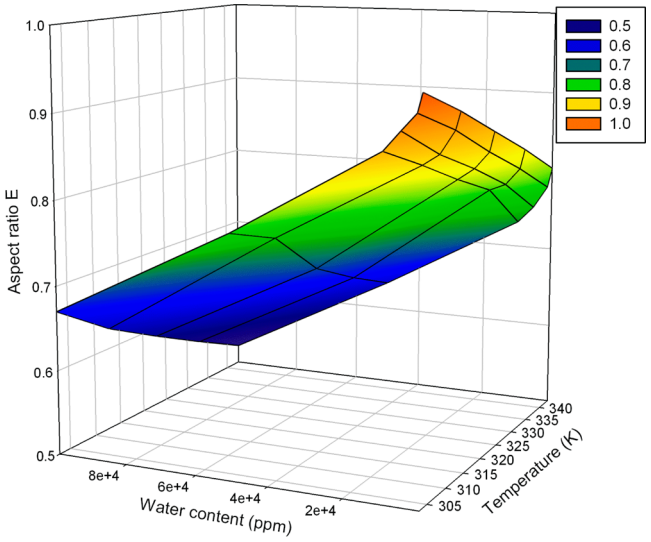

Figure 16. Effect of water content and temperature on bubble deformation in [bmim][BF_4] (Q_{in} = 0.25 mL/min, D_o = 0.47 mm).

3.3.3. Bubble Diameter Correlation. Some models were proposed for calculating the bubble equivalent diameter, d_{eq}. Kumar and Kuloor[42] introduced the concept of two-stage bubble formation for the first time, which was used for explaining the process of bubble formation.

$$d_{eq} = \left[(2\pi)^{0.25} \left(\frac{15\mu_l Q_{in}}{2\rho_l g} \right)^{0.75} \frac{6}{\pi} \right]^{1/3} \quad (28)$$

where d_{eq} is the bubble equivalent diameter, ρ_l is the liquid density, μ_l is the liquid viscosity, and Q_{in} is the gas flow rate.

Wraith[43] showed that the velocity potential could be successfully used in developing a two-stage mechanism for bubble formation and it could be used to calculate the bubble diameter. This model takes into account the growth of bubble accompanied by the change in shape from spherical to hemispherical during expansion before detachment, which can be written as

dx.doi.org/10.1021/ie4020827 | Ind. Eng. Chem. Res. 2014, 53, 428−439

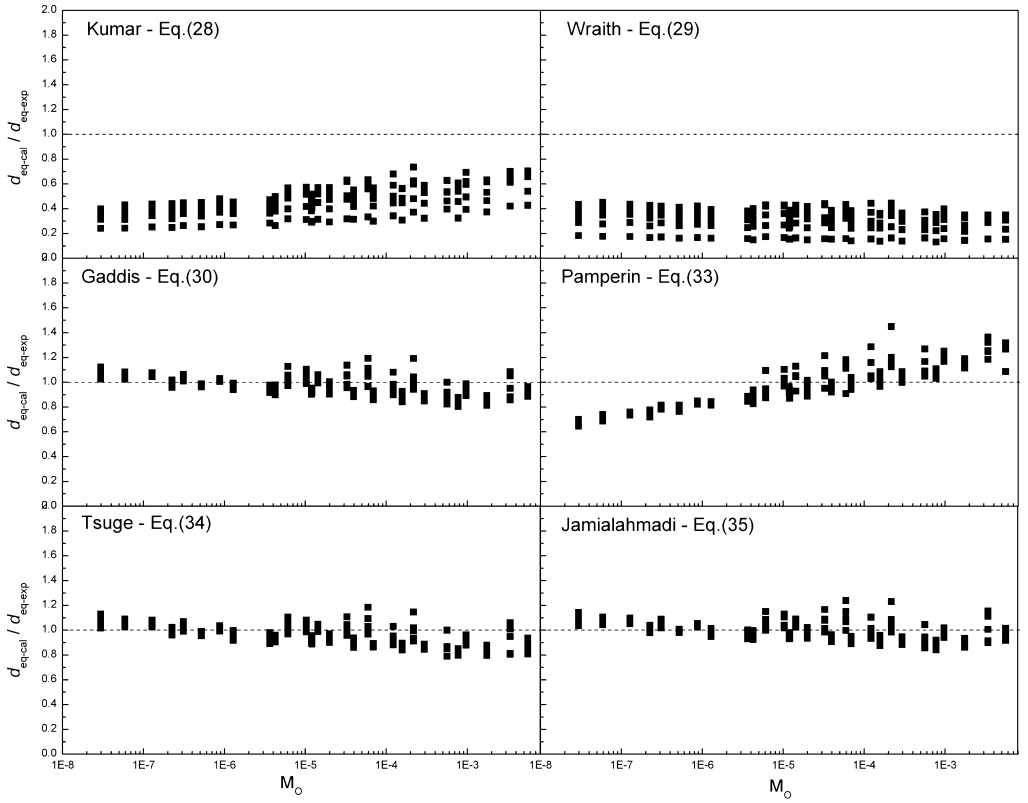

Figure 17. Predictions of bubble equivalent diameter in ionic liquid systems using models from the literature as a function of Morton number.

$$d_{eq} = \left[1.09 Q_{in}^{1.2} g^{-0.6} \frac{6}{\pi}\right]^{1/3} \tag{29}$$

Gaddis and Vogelpohl[44] introduced a simple model for bubble formation in quiescent liquids under constant flow condition, which was valid over a wide range of viscosity and gas flow rates.

$$d_{eq} = \left[\left(\frac{6 D_o \sigma}{\rho_l g}\right)^{4/3} + \frac{81 Q_{in} \mu_l}{\pi g \rho_l} + \left(\frac{135 Q_{in}^2}{4\pi^2 g}\right)^{4/5}\right]^{0.25} \tag{30}$$

Pamperin and Rath[45] investigated the influence of buoyancy on air bubble formation in water at submerged orifices. A model was proposed based on the Reynolds number and the Weber number (in terms of orifice diameter):

$$Re_o = \frac{V_T D_o \rho_l}{\mu_l} \tag{31}$$

$$We_o = \frac{V_T^2 D_o \rho_l}{\sigma} \tag{32}$$

$$d_{eq} = D_o\left[\left(\frac{4}{Re_o} + \frac{0.68}{\sqrt{Re_o}} + 0.183\right)\frac{\rho_l}{\rho_g}\frac{We_o}{We_o - 8}\right]^{1/2} \tag{33}$$

Tsuge et al.[46] studied the two-stage nonspherical bubble formation in quiescent liquid. A new equation was used to predict the bubble diameter at reduced gravity:

$$d_{eq} = \left[\frac{\pi D_o \sigma}{\rho_l g}\frac{6}{\pi}\right]^{1/3} \tag{34}$$

Recently, Jamialahmadi et al.[47] carried out an experimental and theoretical investigation on bubble formation under constant flow conditions. A neural network approach was adopted to handle the nonlinear dependence of various parameters on bubble size.

$$d_{eq} = D_o\left[\frac{5}{Eo_o^{1.08}} + \frac{9.26 Fr_o^{0.36}}{Ga_o^{0.39}} + 2.147 Fr_o^{0.51}\right]^{1/3} \tag{35}$$

where D_o is the orifice diameter, Eo_o is the Eötvös number, Fr_o is the Froude number, and Ga_o is the Galileo number.

Figure 17 shows the predictions of bubble equivalent diameters in ionic liquid systems using previously mentioned models. As shown in Figure 17, the Kumar and Kuloor correlation and the Wraith correlation both present relatively large underestimations for the data in ionic liquid systems, up to −80 and −100%, respectively. The correlations of eqs 30, 34, and 35 show similar tendencies with the entire range of *Mo*, while the Jamialahmadi correlation presents the most proximate estimation with an overestimation within +25% and an underestimation within −20%. Furthermore, eq 33 does not fit the experimental data in ionic liquid systems as well, and shows an overestimation within +50% and an underestimation within −35%.

From the results of Figure 17, the correlations cannot give satisfactory predictions for bubble equivalent diameters in ionic liquid systems. Thus, a new correlation was proposed based on the Froude and Morton dimensionless numbers, which was supposed to have the following form:

dx.doi.org/10.1021/ie4020827 | *Ind. Eng. Chem. Res.* 2014, 53, 428−439

$$d_{eq}\left[\frac{D_o\sigma}{\rho_l g}\right]^{-1/3} = aFr_o^{\,b}Mo^{c} \quad (36)$$

The value of each parameter a, b, and c is acquired by the least-squares method. Then eq 36 can be written as

$$d_{eq}\left[\frac{D_o\sigma}{\rho_l g}\right]^{-1/3} = 2.675Fr_o^{\,0.029}Mo^{0.016} \quad (37)$$

Figure 18 presents the relative deviations between the experimental and calculated bubble equivalent diameters as a function of the experimental bubble diameter. Figure 18 clearly shows that the majority of the deviations are within ±7% and the deviations are distributed randomly around the baseline of 0%, which demonstrates a good application of this correlation in ionic liquid systems.

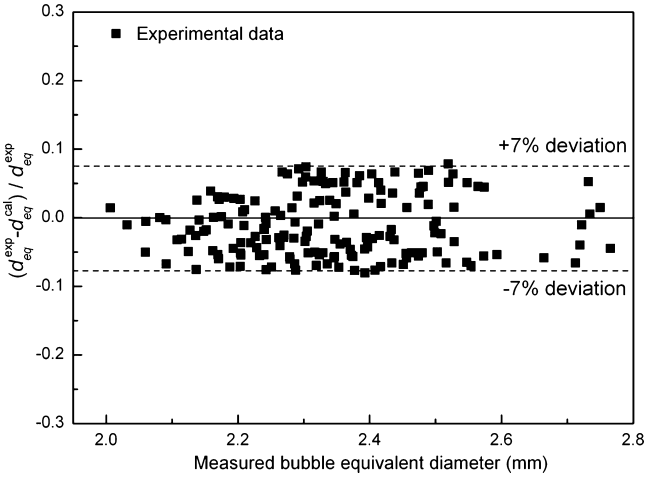

Figure 18. Relative deviations between experimental and calculated bubble equivalent diameters as a function of experimental bubble diameter.

3.3.4. Validation of the New Correlations. The proposed two correlations are based on the experimental data of the aqueous ionic liquid. In order to investigate the validity of the developed correlations in other kinds of ionic liquid systems, ethylene glycol (EG), which is widely used in the chemical industry, was chosen to mix with [bmim][BF_4] to make a verification. The physical properties of the three ionic liquid systems are shown in Table 3. Figure 19 presents the profiles of bubble terminal velocities and bubble equivalent diameters as a function of temperature. It shows that the bubble terminal velocity increases with increasing temperature, namely, with decreasing viscosity. Meanwhile, the bubble equivalent diameter decreases with increasing temperature.

The predicted results of V_T and d_{eq} in the [bmim][BF_4] + 5% EG system calculated by eqs 27 and 37 are listed in Table 4. It shows that the new correlations also present satisfactory predictions for the [bmim][BF_4] + 5% EG system with average relative errors of 5.07% for V_T and 5.92% for d_{eq}, respectively. Thus, it is concluded that the proposed correlations may have a good applicability for different ionic liquid systems.

4. CONCLUSIONS

The single CO_2 bubbles rising in quiescent ionic liquids with varying water contents, gas flow rates, and liquid temperatures were studied using a high speed image pickup system. The bubble velocity, bubble diamter, and bubble shape were determined by analyzing the images. The results demonstrate that a small amount of water has a significant impact on bubble behavior in ionic liquids. Viscosity dominates the bubble behavior in ionic liquid systems compared with surface tension. The bubble velocity increases while bubble diameter and

Table 3. Density (ρ_l), Viscosity (μ_l), and Surface Tension (σ) of Different Ionic Liquid Systems

T (K)	[bmim][BF_4] + 0.02% H_2O	[bmim][BF_4] + 5% EG	[bmim][BF_4] + 5% H_2O
		ρ_l(g/cm^3)	
303	1.198 363	1.191 094	1.182 27
313	1.191 293	1.183 92	1.174 96
323	1.184 268	1.176 804	1.167 732
333	1.177 285	1.169 74	1.160 56
343	1.170 357	1.162 763	1.153 394
		μ_l(mPa s)	
303	87.9756	45.5104	18.9052
313	56.3556	30.6508	13.9495
323	38.3879	21.8239	10.675
333	27.5292	16.23	8.4378
343	19.0732	12.545	6.7694
		σ (mN/m)	
303	44.46	44.14	44.7
313	44.09	43.77	44.33
323	43.66	43.22	43.97
333	43.22	42.71	43.5
343	42.71	42.23	43.01

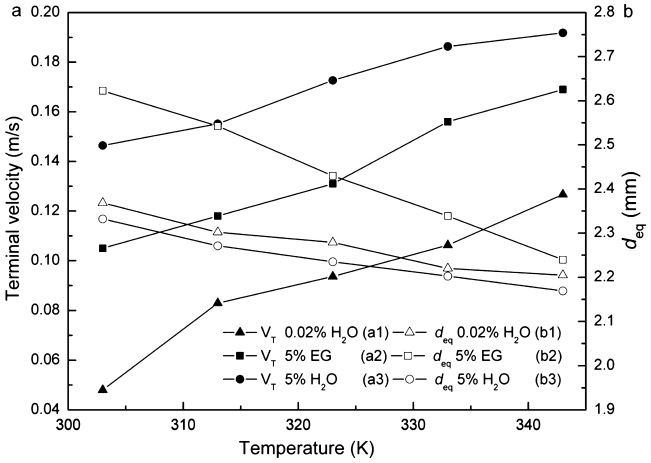

Figure 19. Comparison of bubble terminal velocity and bubble diameter in different ionic liquid systems: (1) 0.02% H_2O, (2) 5% EG, and (3) 5% H_2O (Q_{in} = 0.25 mL/min, D_o = 0.47 mm).

Table 4. Comparison between Experimental and Predicted results of V_T and d_{eq} in [bmim][BF_4] + 5% EG System Using eqs 27 and 37

T (K)	$V_{T\text{-exp}}$ (m/s)	$V_{T\text{-cal}}$ (m/s)	rel error[a]	$d_{eq\text{-exp}}$ (mm)	$d_{eq\text{-cal}}$ (mm)	rel error[a]
303	0.105	0.112	6.67	2.62	2.42	7.63
313	0.119	0.126	5.88	2.54	2.35	7.48
323	0.131	0.139	6.11	2.42	2.29	5.37
333	0.156	0.152	2.56	2.34	2.21	5.55
343	0.169	0.162	4.14	2.23	2.15	3.59

[a]Relative error = (lexp − call)/(exp) × 100%.

dx.doi.org/10.1021/ie4020827 | Ind. Eng. Chem. Res. 2014, 53, 428−439

bubble aspect ratio decrease when the water content in ionic liquids is increased.

Several bubble terminal velocity and bubble diameter correlations available in the literature were used to predict the ionic liquid systems. However, those correlations all show relatively big errors. Two new correlations for predicting bubble terminal velocity and bubble diameter in ionic liquid systems were proposed and tested against experimental data, indicating relative errors within ±10 and ±7%, respectively. Furthermore, the newly proposed correlations were verified in an ionic liquid and EG system, showing an average relative error of less than 6%.

AUTHOR INFORMATION

Corresponding Authors

*Tel.: +86-010-82544875. Fax: +86-010-82544875. E-mail: xpzhang@home.ipe.ac.cn.

*Tel.: +86-010-82544875. Fax: +86-010-82544875. E-mail: sjzhang@home.ipe.ac.cn.

Notes

The authors declare no competing financial interest.

ACKNOWLEDGMENTS

We would like to acknowledge the support from the National Basic Research Program of China (973 Program) (2013CB733506), the Key Program of National Natural Science Foundation of China (No.21036007), and the National Natural Science Foundation of China (No. 51274183).

NOMENCLATURE

d_{eq} = bubble equivalent diameter, mm
d_h = horizontal diameter, mm
D_o = orifice diameter, mm
d_v = vertical diameter, mm
E = bubble aspect ratio, dimensionless
g = gravity acceleration magnitude, m/s^2
L = distance between bubbles, m
Q_{in} = gas flow rate, mL/min
T = temperature, K
U_g = gas superficial velocity, m/s
V_i = bubble local velocity, m/s
V_T = bubble terminal velocity, m/s
x_i = horizontal coordinate of the bubble
y_i = vertical coordinate of the bubble

Dimensionless Numbers in Terms of Bubble Diameter

Ca = capillary number, $Ca = \mu_l V_T/\sigma$
Eo = Eötvös number, $Eo = \rho_l g d_{eq}^2/\sigma$
F = flow number, $F = Eo \cdot Re^{2/3}/Ca^{2/3}$
Mo = Morton number, $Mo = g\mu_l^4(\rho_l - \rho_g)/\sigma^3\rho_l^2$
Re = Reynolds number, $Re = \rho_l V_T d_{eq}/\mu_l$
U = velocity number, $U = (Re^2 Ca)^{1/3}$

Dimensionless Numbers in Terms of Orifice Diameter

Eo_o = Eötvös number, $Eo_o = D_o^2\rho_l g/\sigma$
Fr_o = Froude number, $Fr_o = U_g^2/D_o g$
Ga_o = Galileo number, $Ga_o = D_o^3\rho_l^2 g/\mu_l^2$
Re_o = Reynolds number, $Re_o = V_T D_o \rho_l/\mu_l$
We_o = Weber number, $We_o = V_T^2 D_o \rho_l/\sigma$

Greek Symbols

σ = surface tension, N/m
μ = viscosity, Pa s
ρ = density, kg/m^3

Subscripts

cal = calculated value
exp = experimental value
g = gas
l = liquid
o = orifice

REFERENCES

(1) Bishnoi, S.; Rochelle, G. T. Absorption of carbon dioxide into aqueous piperazine: reaction kinetics, mass transfer and solubility. *Chem. Eng. Sci.* **2000**, *55*, 5531−5543.

(2) Camacho, F.; Sanchez, S.; Pacheco, R. Absorption of carbon dioxide at high partial pressures in 1-amino-2-propanol aqueous solution. Considerations of thermal effects. *Ind. Eng. Chem. Res.* **1997**, *36*, 4358−4364.

(3) Paul, S.; Ghoshal, A. K.; Mandal, B. Absorption of carbon dioxide into aqueous solutions of 2-piperidineethanol: Kinetics analysis. *Ind. Eng. Chem. Res.* **2009**, *48*, 1414−1419.

(4) Rinker, E. B.; Ashour, S. S.; Sandall, O. C. Absorption of carbon dioxide into aqueous blends of diethanolamine and methyldiethanolamine. *Ind. Eng. Chem. Res.* **2000**, *39*, 4346−4356.

(5) Gurkan, B. E.; de la Fuente, J. C.; Mindrup, E. M.; Ficke, L. E.; Goodrich, B. F.; Price, E. A.; Schneider, W. F.; Brennecke, J. F. Equimolar CO_2 absorption by anion-functionalized ionic liquids. *J. Am. Chem. Soc.* **2010**, *132*, 2116−2117.

(6) Bara, J. E.; Carlisle, T. K.; Gabriel, C. J.; Camper, D.; Finotello, A.; Gin, D. L.; Noble, R. D. Guide to CO_2 separations in imidazolium-based room-temperature ionic liquids. *Ind. Eng. Chem. Res.* **2009**, *48*, 2739−2751.

(7) MacDowell, N.; Florin, N.; Buchard, A.; Hallett, J.; Galindo, A.; Jackson, G.; Adjiman, C. S.; Williams, C. K.; Shah, N.; Fennell, P. An overview of CO_2 capture technologies. *Energy Environ. Sci.* **2010**, *3*, 1645−1669.

(8) Zhang, X. P.; Zhang, X. C.; Dong, H. F.; Zhao, Z. J.; Zhang, S. J.; Huang, Y. Carbon capture with ionic liquids: overview and progress. *Energy Environ. Sci.* **2012**, *5*, 6668−6681.

(9) Gutowski, K. E.; Maginn, E. J. Amine-functionalized task-specific ionic liquids: a mechanistic explanation for the dramatic increase in viscosity upon complexation with CO_2 from molecular simulation. *J. Am. Chem. Soc.* **2008**, *130*, 14690−14704.

(10) Zhang, J. M.; Zhang, S. J.; Dong, K.; Zhang, Y. Q.; Shen, Y. Q.; Lv, X. M. Supported absorption of CO_2 by tetrabutylphosphonium amino acid ionic liquids. *Chem.—Eur. J.* **2006**, *12*, 4021−4026.

(11) Zhang, L. L.; Wang, J. X.; Xiang, Y.; Zeng, X. F.; Chen, J. F. Absorption of carbon dioxide with ionic liquid in a rotating packed bed contactor: Mass transfer study. *Ind. Eng. Chem. Res.* **2011**, *50*, 6957−6964.

(12) Seddon, K. R.; Stark, A.; Torres, M. J. Influence of chloride, water, and organic solvents on the physical properties of ionic liquids. *Pure Appl. Chem.* **2000**, *72*, 2275−2287.

(13) Goodrich, B. F.; de la Fuente, J. C.; Gurkan, B. E.; Lopez, Z. K.; Price, E. A.; Huang, Y.; Brennecke, J. F. Effect of water and temperature on absorption of CO_2 by amine-functionalized anion-tethered ionic liquids. *J. Phys. Chem. B* **2011**, *115*, 9140−9150.

(14) Wang, Z. X.; Fu, L.; Xu, H.; Shang, Y.; Zhang, L.; Zhang, J. M. Density, viscosity, and conductivity for the binary systems of water plus dual amino-functionalized ionic liquids. *J. Chem. Eng. Data* **2012**, *57*, 1057−1063.

(15) Ruzicka, M. C.; Bunganic, R.; Drahos, J. Meniscus dynamics in bubble formation. Part I: Experiment. *Chem. Eng. Res. Des.* **2009**, *87*, 1349−1356.

(16) Alves, S. S.; Orvalho, S. P.; Vasconcelos, J. M. T. Effect of bubble contamination on rise velocity and mass transfer. *Chem. Eng. Sci.* **2005**, *60*, 1−9.

(17) Celata, G. P.; D'Annibale, F.; Di Marco, P.; Memoli, G.; Tomiyama, A. Measurements of rising velocity of a small bubble in a stagnant fluid in one-and two-component systems. *Exp. Therm. Fluid Sci.* **2007**, *31*, 609−623.

(18) Parkinson, L.; Sedev, R.; Fornasiero, D.; Ralston, J. The terminal rise velocity of 10−100 μm diameter bubbles in water. *J. Colloid Interface Sci.* **2008**, *322*, 168−172.
(19) Maxworthy, T.; Gnann, C.; Kürten, M.; Durst, F. Experiments on the rise of air bubbles in clean viscous liquids. *J. Fluid Mech.* **1996**, *321*, 421−441.
(20) Snabre, P.; Magnifotcham, F. I. Formation and rise of a bubble stream in a viscous liquid. *Eur. Phys. J. B* **1998**, *4*, 369−377.
(21) Kawahara, A.; Sadatomi, M.; Nei, K.; Matsuo, H. Experimental study on bubble velocity, void fraction and pressure drop for gas-liquid two-phase flow in a circular microchannel. *Int. J. Heat Fluid Flow* **2009**, *30*, 831−841.
(22) Terasaka, K.; Tsuge, H. Bubble formation at a nozzle submerged in viscous liquids having yield stress. *Chem. Eng. Sci.* **2001**, *56*, 3237−3245.
(23) Pancholi, K.; Stride, E.; Edirisinghe, M. Dynamics of bubble formation in highly viscous liquids. *Langmuir* **2008**, *24*, 4388−4393.
(24) Dong, H. F.; Wang, X. L.; Liu, L.; Zhang, X. P.; Zhang, S. J. The rise and deformation of a single bubble in ionic liquids. *Chem. Eng. Sci.* **2010**, *65*, 3240−3248.
(25) Wang, X. L.; Dong, H. F.; Zhang, X. P.; Xu, Y.; Zhang, S. J. Numerical simulation of absorbing CO_2 with ionic liquids. *Chem. Eng. Technol.* **2010**, *33*, 1615−1624.
(26) Wang, X. L.; Dong, H. F.; Zhang, X. P.; Yu, L.; Zhang, S. J.; Xu, Y. Numerical simulation of single bubble motion in ionic liquids. *Chem. Eng. Sci.* **2010**, *65*, 6036−6047.
(27) Zhang, X.; Dong, H. F.; Huang, Y.; Li, C. S.; Zhang, X. P. Experimental study on gas holdup and bubble behavior in carbon capture systems with ionic liquid. *Chem. Eng. J.* **2012**, *209*, 607−615.
(28) Nedeltchev, S.; Jordan, U.; Schumpe, A. Correction of the penetration theory based on mass-transfer data from bubble columns operated in the homogeneous regime under high pressure. *Chem. Eng. Sci.* **2007**, *62*, 6263−6273.
(29) Spohr, H. V.; Patey, G. N. The influence of water on the structural and transport properties of model ionic liquids. *J. Chem. Phys.* **2010**, *132*, 234510.
(30) Zhang, S.; Sun, N.; He, X.; Lu, X.; Zhang, X. Physical properties of ionic liquids: database and evaluation. *J. Phys. Chem. Ref. Data* **2006**, *35*, 1475−1517.
(31) Kulkarni, P. S.; Branco, L. C.; Crespo, J. G.; Nunes, M. C.; Raymundo, A.; Afonso, C. A. Comparison of physicochemical properties of new ionic liquids based on imidazolium, quaternary ammonium, and guanidinium cations. *Chem.—Eur. J.* **2007**, *13*, 8478−8488.
(32) Mendelson, H. D. The prediction of bubble terminal velocities from wave theory. *AIChE J.* **1967**, *13*, 250−253.
(33) Fan, L. S.; Tsuchiya, K. *Bubble Wake Dynamics in Liquids and Liquid-Solid Suspensions*; Butterworth-Heinemann: Oxford, U.K., 1990.
(34) Jamialahmadi, M.; Branch, C.; Müller-Steinhagen, H. Terminal bubble rise velocity in liquids. *Chem. Eng. Res. Des.* **1994**, *72*, 119−122.
(35) Rodrigue, D. Generalized correlation for bubble motion. *AIChE J.* **2004**, *47*, 39−44.
(36) Tomiyama, A.; Celata, G.; Hosokawa, S.; Yoshida, S. Terminal velocity of single bubbles in surface tension force dominant regime. *Int. J. Multiphase Flow* **2002**, *28*, 1497−1519.
(37) Cai, Z. Q.; Bao, Y. Y.; Gao, Z. M. Hydrodynamic behavior of a single bubble rising in viscous liquids. *Chin. J. Chem. Eng.* **2010**, *18*, 923−930.
(38) Law, G.; Watson, P. R.; Carmichael, A. J.; Seddon, K. R. Molecular composition and orientation at the surface of room-temperature ionic liquids: Effect of molecular structure. *Phys. Chem. Chem. Phys.* **2001**, *3*, 2879−2885.
(39) Kulkarni, A. A.; Joshi, J. B. Bubble formation and bubble rise velocity in gas-liquid systems: A review. *Ind. Eng. Chem. Res.* **2005**, *44*, 5873−5931.
(40) Sardeing, R.; Painmanakul, P.; Hébrard, G. Effect of surfactants on liquid-side mass transfer coefficients in gas−liquid systems: a first step to modeling. *Chem. Eng. Sci.* **2006**, *61*, 6249−6260.
(41) Oyenekan, B. A.; Rochelle, G. T. Energy performance of stripper configurations for CO_2 capture by aqueous amines. *Ind. Eng. Chem. Res.* **2006**, *45*, 2457−2464.
(42) Kumar, R.; Kuloor, N. The formation of bubbles and drops. *Adv. Chem. Eng.* **1970**, *8*, 255−368.
(43) Wraith, A. Two stage bubble growth at a submerged plate orifice. *Chem. Eng. Sci.* **1971**, *26*, 1659−1671.
(44) Gaddis, E.; Vogelpohl, A. Bubble formation in quiescent liquids under constant flow conditions. *Chem. Eng. Sci.* **1986**, *41*, 97−105.
(45) Pamperin, O.; Rath, H. J. Influence of buoyancy on bubble formation at submerged orifices. *Chem. Eng. Sci.* **1995**, *50*, 3009−3024.
(46) Tsuge, H.; Tanaka, Y.; Terasaka, K.; Matsue, H. Bubble formation in flowing liquid under reduced gravity. *Chem. Eng. Sci.* **1997**, *52*, 3671−3676.
(47) Jamialahmadi, M.; Zehtaban, M.; Müller-Steinhagen, H.; Sarrafi, A.; Smith, J. Study of bubble formation under constant flow conditions. *Chem. Eng. Res. Des.* **2001**, *79*, 523−532.